Magnetic susceptibilities of V^{3+} in corundum: Magnetic anisotropy at high fields

William H. Brumage*
1802 Saddleback Boulevard, Norman, Oklahoma 73072

C. Richard Quade
Department of Physics, Texas Tech University, Lubbock, Texas 79409

C. Franklin Dorman
Division of Science, University of Science and Arts of Oklahoma, Chickasha, Oklahoma 73018
(Received 27 February 1995)

We theoretically investigate the behavior of the V^{3+} ion as an impurity in Al_2O_3 under high magnetic fields, up to 20 T. In particular, we investigate the introduction of magnetic anisotropy that is lower than the trigonal symmetry of the host crystal. Two approaches are used for the calculations. First, fourth-order perturbation theory is used to develop quartic terms plus one sextic term in the susceptibility tensor that are good for fields up to 4 T. Then, the three-level energy matrix is reduced exactly to obtain the anisotropy at higher fields. It is found that the dominant contributions to the magnetic-induced anisotropy arise from the χ_{xxxx} term, while the $\chi_{xxzz}=\chi_{zxxz}$, χ_{zzzz}, and the χ_{xxxxxx} terms give a much lower contribution. Temperature-dependent effects are reported. There is a very small dependence of the magnetization upon the zero-field splitting.

INTRODUCTION

Many years ago we theoretically and experimentally investigated the magnetic susceptibilities of impurity ions in host crystals for systems of differing symmetry.[1] In all of these cases the systems were studied under weak magnetic fields. That is, the susceptibility tensor was taken to second rank and it was diagonal in a coordinate system that corresponded to the symmetry of the crystal.

Villeret *et al.*[2] have investigated the magnetic properties of certain cubic systems under strong magnetic fields. In the case of strong magnetic fields, additional anisotropy is introduced by the field. The magnetic susceptibility tensor must be considered to terms higher than second rank and the tensor no longer is diagonal in a coordinate system that corresponds to the symmetry of the crystal without the applied field. Essentially, Villeret *et al.* studied how the bulk magnetization relative to the magnetic field varied with specific directions chosen in the samples. For these magnetic anisotropy effects to be observable, the magnetic energy must be comparable to the crystal-field splittings and/or the spin-orbit splittings. The systems reported have unusually weak cubic crystalline fields and the spin-orbit coupling is consistent with that of other $3d$ electron systems. Recently Fries *et al.*[3] have reported measurements and calculations of magnetic anisotropy in cubic $Z_{1-x}Fe_xSe$. An interesting feature of this system is that for the crystal directions chosen, although the magnetization varies with applied field, the magnetization remains parallel to the field.

In this work we revisit one of the systems that we studied previously under weak magnetic fields—V^{3+} as an impurity ion in the host Al_2O_3. For this ion both the cubic and the trigonal crystal-field energies are large compared to the magnetic energies of even 15 to 20 T. The ground state $^3A_2$ level of the trigonal field is split in second order by the spin-orbit interaction into a spin singlet 8.25 cm^{-1} below a spin doublet. This spin-orbit splitting is unperturbed by magnetic fields of 20 T. The splitting is small enough so that magnetic anisotropy lower than trigonal is introduced into the susceptibility tensor in higher rank than second for strong magnetic fields. In the present work we investigate the magnetic anisotropy for this three-level system.

Our approach to the susceptibility tensor is different from that introduced by Villeret *et al.*[2] Since, even in the case of strong magnetic fields, the trigonal energy cannot be quenched for the V^{3+}:Al_2O_3 system, we chose a coordinate system for the susceptibility tensor that corresponds to the trigonal axes. That is, the z axis is taken along the trigonal axis and the x axis is one of the two perpendicular axes. In this coordinate system, the second-rank susceptibility remains diagonal, while the higher rank terms have both diagonal and off-diagonal components. Our approach expands the susceptibility tensor as

$$\overline{M}_i=\sum\chi_{ij}H_j+\sum\chi_{ijk}H_jH_k+\sum\chi_{ijkl}H_jH_kH_l+\cdots\ , \tag{1}$$

where $\overline{M}_i$ is the thermal average of the ith component of the magnetic moment. Even in strong magnetic fields, sufficient symmetry remains so that the only nonvanishing coefficients for V^{3+}:Al_2O_3 are

$$\chi_{ij}=\chi_{ii}\delta_{ij}\ ,\quad \chi_{xxxx},\ \chi_{zzzz}\ , \tag{2}$$

and

 ©1995 The American Physical Society

$$\chi_{xxzz}=\chi_{zxxz}$$

to fourth rank. We have also found it necessary to include the χ_{xxxxxx} term.

In magnetic-susceptibility measurements, often the individual components of the susceptibilities or magnetizations are measured separately. At other times a sample is oriented so that the magnetic field is in the x-z plane which causes a torque on the sample. Then

$$\underline{N}=\underline{\overline{M}}\times\underline{H} \tag{3}$$

or

$$N_y=\overline{M}_z H_x-\overline{M}_x H_z \tag{4}$$

in terms of the susceptibility coefficients, $N_y(=N)$ becomes

$$N=[(\chi_{zz}-\chi_{xx})+(\chi_{zxxz}-\chi_{xxxx})H_x^2 +(\chi_{zzzz}-\chi_{xxzz})H_z^2-(\chi_{xxxxxx})H_x^4]H_xH_z\ . \tag{5}$$

In this work we use two methods of calculation. The first is a perturbation approach that goes through fourth order in the magnetic field for the magnetic energies. Formulas for the temperature-dependent magnetic susceptibility coefficients χ_{xx}, χ_{zz}, χ_{xxxx}, χ_{zzzz}, $\chi_{xxzz}=\chi_{zxxz}$, and χ_{xxxxxx} are developed. The perturbation approach is good for fields up to 4 T. The second approach uses an analytical diagonalization of the energy matrix with an accompanying development of the magnetic moment. In this approach it has not been possible to develop closed formulas for the susceptibility coefficients; however, the results are instructively presented through graphs of the numerical results. In this approach fields up to 20 T are considered which remain low enough so as not to perturb the 8.25 cm^{-1} zero-field splitting.

In our calculation we neglect the second-order Van Vleck susceptibility that arises from the interaction of the $^3A_2(^3T_1)$ ground-state levels with the $^3E(^3T_1)$ and the $^3T_2$ levels.[1(a)] Although these terms are not zero, they are small and would contribute less than 1% to the calculated results at the temperatures and fields under consideration.

The energy-level system for the $(3d)^2$ electron configuration of V^{3+}:Al_2O_3 in the cubic and trigonal crystalline fields is given in Fig. 1. Some of the critical energy differences are $\delta=8.25$ cm^{-1}, $\Delta_T=1100$ cm^{-1}, and $\Delta_c=17\,400$ cm^{-1}. Again, δ arises from a second-order spin-orbit coupling interaction predominantly of $^3A_2(T_1)$ with $^3E(T_1)$. The spin-orbit coupling coefficient λ was found to be of the order 95 cm^{-1} for the V^{3+} ion in the Al_2O_3 host crystal.[1(a)] For magnetic fields less than 20 T, δ is not influenced by the magnetic fields.

PERTURBATION APPROACH

The magnetic interaction for the V^{3+}:Al_2O_3 system is easily reduced to a three-level system that has the form

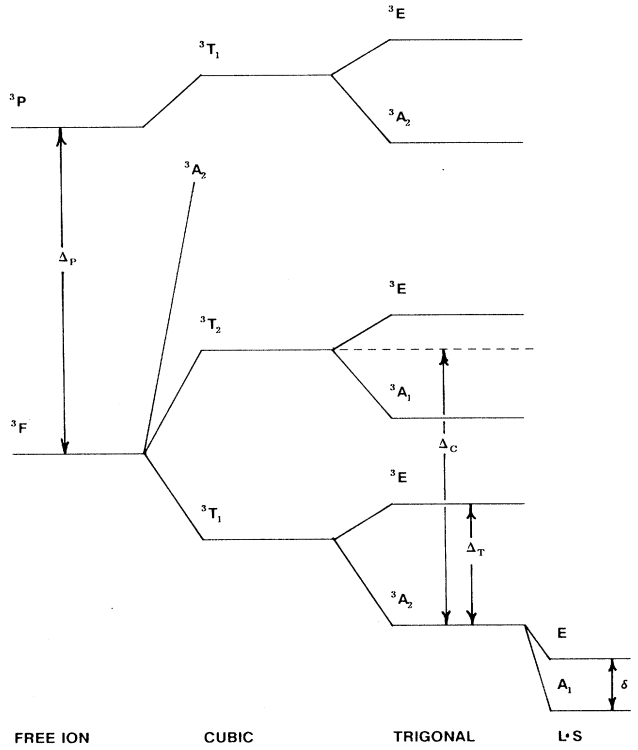

FIG. 1. Energy levels of V^{3+} in a trigonal field.

$M_s \backslash M_s$	0	−1	+1
0	0	$g_\perp\mu_0 H_x/\sqrt{2}$	$g_\perp\mu_0 H_x/\sqrt{2}$
−1		$\delta-g_\parallel\mu_0 H_z$	0
+1			$\delta+g_\parallel\mu_0 H_z$

(6)

where μ_0 is the Bohr magnetron, $g_\parallel$, $g_\perp$, and δ have been determined from electron-spin resonance[4] and infrared spectroscopy,[6] respectively, and depend upon the crystal-field parameters and spin-orbit coupling constant. To fourth order H_z and sixth order in H_x

$$\begin{aligned} E_0&=-AH_x^2+BH_x^4-CH_x^2H_z^2-GH_x^6\ ,\\ E_{+1}&=DH_z+\tfrac{1}{2}AH_x^2-FH_x^2H_z-\tfrac{1}{2}BH_x^4+\tfrac{1}{2}CH_x^2H_z^2\\ &\quad+\tfrac{1}{2}GH_x^6+\delta\ ,\\ E_{-1}&=-DH_z+\tfrac{1}{2}AH_x^2+FH_x^2H_z-\tfrac{1}{2}BH_x^4+\tfrac{1}{2}CH_x^2H_z^2\\ &\quad+\tfrac{1}{2}GH_x^6+\delta\ , \end{aligned} \tag{7}$$

where

$$\begin{aligned} &A=g_\perp^2\mu_0^2/\delta,\quad B=g_\perp^4\mu_0^4/\delta^3\ ,\\ &C=g_\perp^2g_\parallel^2\mu_0^4/\delta^3,\quad D=g_\parallel\mu_0\ ,\\ &F=g_\perp^2g_\parallel\mu_0^3/2\delta^2,\quad G=2g_\perp^6\mu_0^6/\delta^5\ . \end{aligned} \tag{8}$$

The magnetic moment is given by[5]

$$m_i(n) = -\partial E_n / \partial H_i \ . \tag{9}$$

Further, the temperature-dependent magnetic moment $\overline{M}$ is given by

$$\overline{M}_i = \frac{\sum m_i(n) e^{-En/kT}}{\sum e^{-En/kT}} \ . \tag{10}$$

The temperature-dependent susceptibility coefficients, Eq. (2), have been calculated using Eqs. (7), (9), and (10) and are as follows:

$$\begin{aligned}
\chi_{xx} &= (1+2e^{-\delta/kT})^{-1} 2A(1-e^{-\delta/kT}) \ , \\
\chi_{zz} &= (1+2e^{-\delta/kT})^{-1} 2D^2 e^{-\delta/kT}/kT \ , \\
\chi_{xxxx} &= (1+2e^{-\delta/kT})^{-1}\{-4B(1-e^{-\delta/kT}) + A^2[(2+e^{-\delta/kT}) - 2(1-e^{-\delta/kT})^2(1+2e^{-\delta/kT})^{-1}]/kT\} \ , \\
\chi_{zzzz} &= (1+2e^{-\delta/kT})^{-1}\{[\tfrac{1}{3} - 2e^{-\delta/kT}(1+2e^{-\delta/kT})^{-1}] D^4 e^{-\delta/kT}/(kT)^3\} \ , \\
\chi_{xxzz} = \chi_{zxxz} &= (1+2e^{-\delta/kT})^{-1}([2C(1-e^{-\delta/kT}) - 4DFe^{-\delta/kT}/kT] \\
&\quad - \{D^2 A e^{-\delta/kT}[1+2(1+2e^{-\delta/kT})^{-1}(1-e^{-\delta/kT})]/(kT)^2\}) \ , \\
\chi_{xxxxxx} &= (1+2e^{-\delta/kT})^{-1}\{6G(1-e^{-\delta/kT}) + 3AB[2(1+2e^{-\delta/kT})^{-1}(1-e^{-\delta/kT})^2 - (2+e^{-\delta/kT})]/kT \\
&\quad + \tfrac{1}{4} A^3[(4-e^{-\delta/kT}) - 6(1+2e^{-\delta/kT})^{-1}(1-e^{-\delta/kT})(2+e^{-\delta/kT}) \\
&\quad + 8(1+2e^{-\delta/kT})^{-2}(1-e^{-\delta/kT})^3]/(kT)^2\} \ .
\end{aligned} \tag{11}$$

In Eqs. (11) series expansions have been made for the case of the magnetic energy less than kT. All terms that contribute to the χ's in Eqs. (11) have been kept. Equations (11) are good down to temperatures of 4.2 K and for magnetic fields up to 4 T. The limitations of Eqs. (11) are illustrated under comparison of the results from a more rigorous calculation in a later section of this work. A comparison of the fourth-order energies with the "exact" results developed in the next section are calculated for magnetic fields up to 8 T and are shown in Fig. 2.

There is a second- and fourth-order matrix element, $(-1|H'|+1)$, with quadratic and quartic contributions in H_x that has not been included in this part of the calculation. Neglect of the mixing from this term introduces a 2% error in the application of Eq. (11) to M_x at 77 K and 0.6% error at 5 K for $H_x = 4$ T. Inclusion of this term does not lend itself to the expansion of $m_i(n)$ in a power series in H_x and H_z.

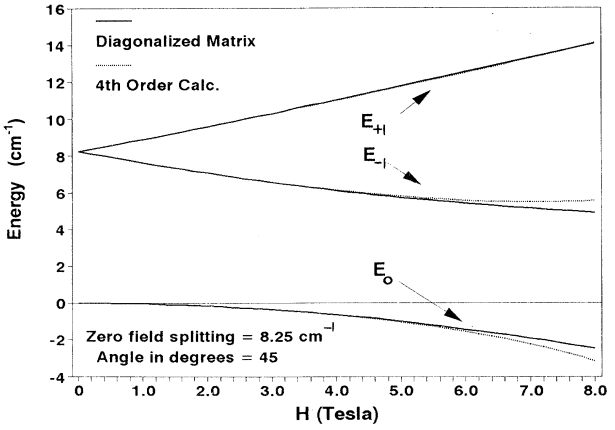

FIG. 2. A comparison of the perturbation and exact energy eigenvalues, Eqs. (7) and (12), up to 8 T.

EXACT REDUCTION OF THE ENERGY MATRIX

Algebraic expressions for the eigenvalues of Eq. (6) may be expressed as

$$\begin{aligned}
\lambda_1 &= \tfrac{2}{3}\delta - 2R^{1/3}\cos(\theta/3) \ , \\
\lambda_2 &= \tfrac{2}{3}\delta + R^{1/3}\cos(\theta/3) + \sqrt{3}R^{1/3}\sin(\theta/3) \ , \\
\lambda_3 &= \tfrac{2}{3}\delta + R^{1/3}\cos(\theta/3) - \sqrt{3}R^{1/3}\sin(\theta/3) \ ,
\end{aligned} \tag{12}$$

where

$$\begin{aligned}
\cos\theta &= \Psi/R \ , \\
\Psi &= (1/27)[\delta^3 - 9\delta g_{\parallel}^2 \mu_0^2 H_z^2 + (9/2)\delta g_{\perp}^2 \mu_0^2 H_x^2] \ , \\
R &= (1/27) Y^{1/2} \ , \\
Y &= \delta^6 + 27 g_{\parallel}^6 \mu_0^6 H_z^6 + 27 g_{\perp}^6 \mu_0^6 H_x^6 + 9\delta^4 g_{\parallel}^2 \mu_0^2 H_z^2 \\
&\quad + 27\delta^2 g_{\parallel}^4 \mu_0^4 H_z^4 + 27\delta^2 g_{\perp}^4 \mu_0^4 H_x^4 + 9\delta^4 g_{\perp}^2 \mu_0^2 H_x^2 \\
&\quad + 81 g_{\perp}^2 g_{\parallel}^4 \mu_0^6 H_x^2 H_z^4 + 81 g_{\perp}^4 g_{\parallel}^2 \mu_0^6 H_x^4 H_z^2 \\
&\quad + 54\delta^2 g_{\perp}^2 g_{\parallel}^2 \mu_0^4 H_x^2 H_z^2 \ .
\end{aligned} \tag{13}$$

Equations (12) and (13) are then used to calculate the matrix elements of the magnetic moment with the result

$$
\begin{aligned}
m_i(1)&=(1/2187)R^{-5/3}\cos(\theta/3)(\partial Y/\partial H_i)+\tfrac{2}{3}R^{1/3}\sin(\theta/3)\\
&\quad\times(1-\Psi^2/R^2)^{-1/2}[(1/R)\partial\Psi/\partial H_i-(\Psi/1458R^3)\partial Y/\partial H_i]\,,\\
m_i(2/3)&=-(1/4374)R^{-5/3}[\cos(\theta/3)\pm\sqrt{3}\sin(\theta/3)](\partial Y/\partial H_i)-\tfrac{1}{3}R^{1/3}[\sin(\theta/3)\mp\sqrt{3}\cos(\theta/3)]\\
&\quad\times(1-\Psi^2/R^2)^{-1/2}[(1/R)\partial\Psi/\partial H_i-(\Psi/1458R^3)\partial Y/\partial H_i]\,.
\end{aligned}
\tag{14}
$$

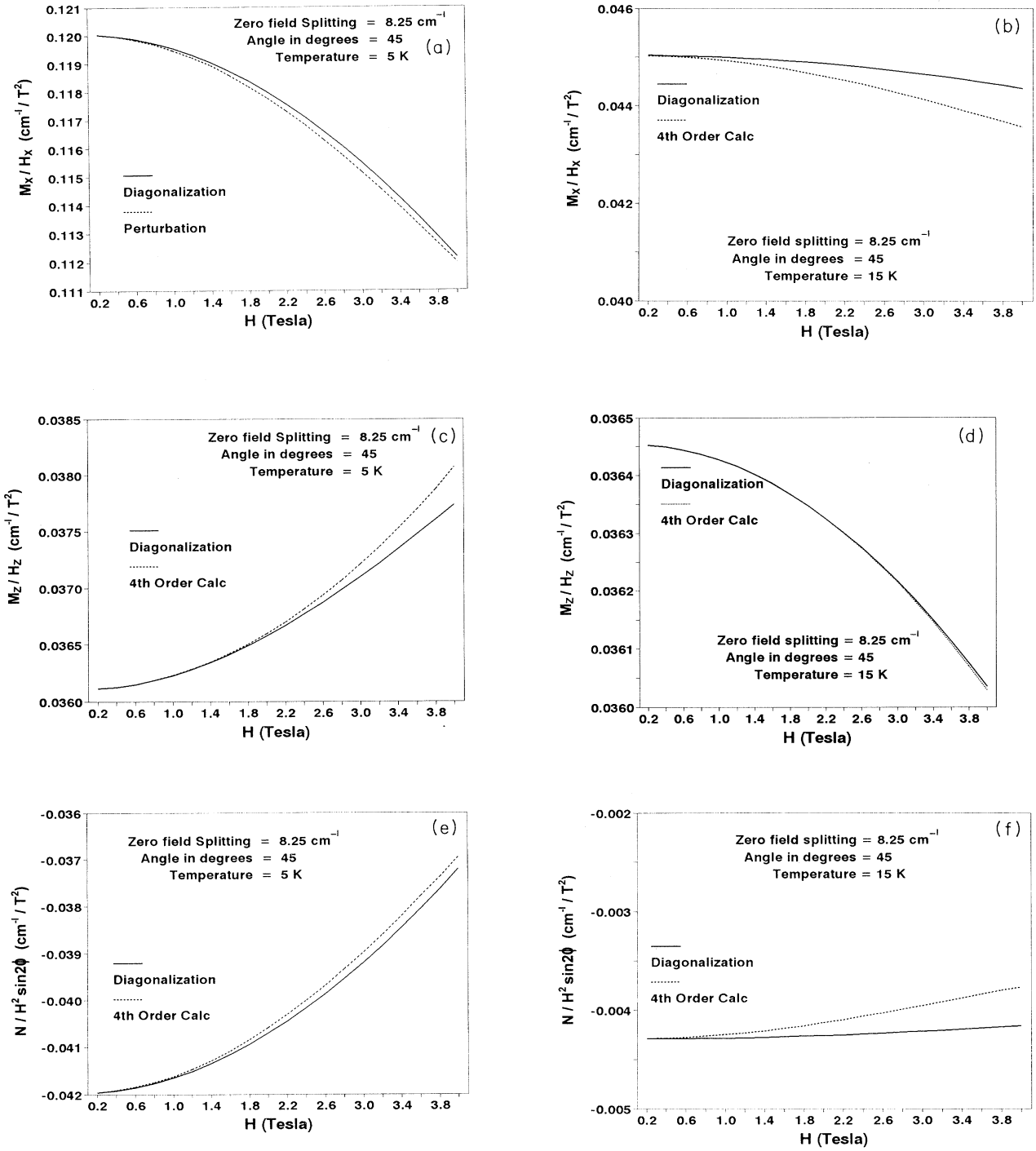

FIG. 3. Dependence of $\overline{M}_x/H_x$, $\overline{M}_z/H_z$, and $N/H^2\sin2\phi$ upon magnetic-field strength H. Comparison of the exact calculation with the perturbation/kT expansion for fields up to 4 T.

To calculate the temperature-dependent magnetic moments, Eqs. (12) and (14) are used with Eq. (10). The results of the calculations are presented in the next section.

CALCULATED RESULTS

Using the formalism of the previous two sections we have calculated the magnetizations $\overline{M}_x$ and $\overline{M}_z$ and the torque N for the V^{3+}:Al_2O_3 system. To illustrate the magnetic-induced anisotropy, calculations are made at different ϕ, the orientation of the magnetic field with respect to the trigonal z axis, for magnetic fields up to 20 T, for different zero-field splittings δ, and for temperatures 1 to 20 K.

Calculations are first made of $\overline{M}_x/H_x$ and $\overline{M}_z/H_z$. In

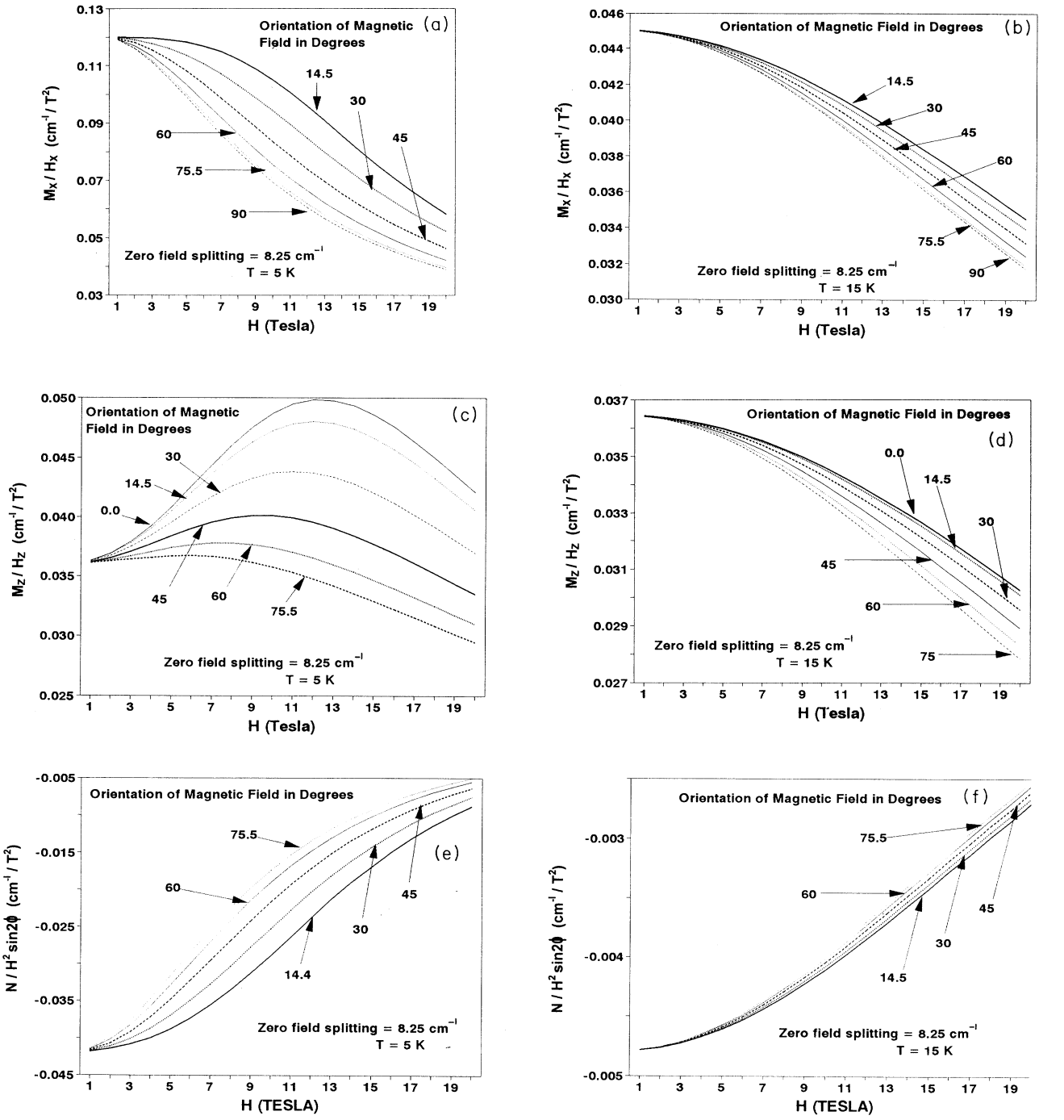

FIG. 4. Dependence of $\overline{M}_x/H_x$, $\overline{M}_z/H_z$, and $N/H^2\sin 2\phi$ upon the orientation of the magnetic field with the crystal trigonal z axis, ϕ, first at 5 K and then at 15 K.

the absence of saturation and magnetic-induced anisotropy, both quantities should be independent of the field strength H. Likewise $N/H^2\sin 2\phi$ should be independent of H.

Figure 3 illustrates a comparison of the results from the perturbation/kT expansion formalism with those from the "exact" calculations at 45°, that is with $H_x = H_z$. The agreement between the two is very good up to 3 T and fair up to 4 T. When appropriate, the perturbation calculations are used since the algebraic expressions are easily evaluated and because of the physical insight offered. These figures clearly illustrate that the perturbation technique and series expansion in kT is a much better approximation for the z terms than for the x terms. In the torque calculation the x terms dominate the divergence of the approximate fourth-order calculation from the "exact" results.

Figure 4 illustrates how $\overline{M}_x/H_x$, etc. vary with orientation of the magnetic field. The magnetic-induced anisotropy and saturation is substantial for fields above 1 T at 5 K. The results for 15 K show that these effects are decreasing with higher temperature.

Figure 5 illustrates the temperature dependence of $\overline{M}_x/H_x$, $\overline{M}_z/H_z$, and $N/H^2\sin 2\phi$ upon the zero-field splitting δ. At low fields both $\overline{M}_x/H_x$ and $\overline{M}_z/H_z$ show a small dependence on δ that disappears at high magnetic fields. However, the dependence of the torque N upon δ is relatively constant over all fields.

Figure 6 illustrates the temperature dependence of $\overline{M}_x/H_x$, etc. This dependence for several fields is included at 45°. At low temperatures there is a strong field effect whereas at high temperature, greater than 20 K, the field dependence disappears. This is a well-known phenomenon—the saturation and anisotropy terms in $m_i(n)$ cancel with those from the E_n when the magnetic energy is much less than kT in the calculated M_i.

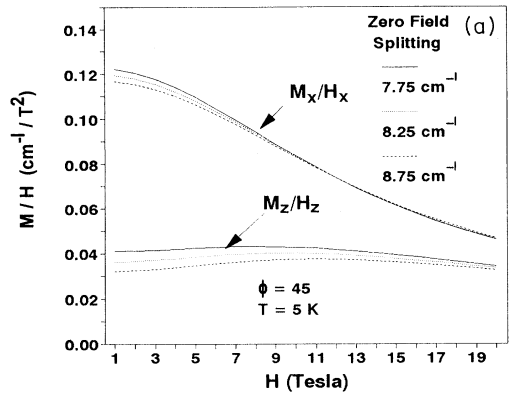

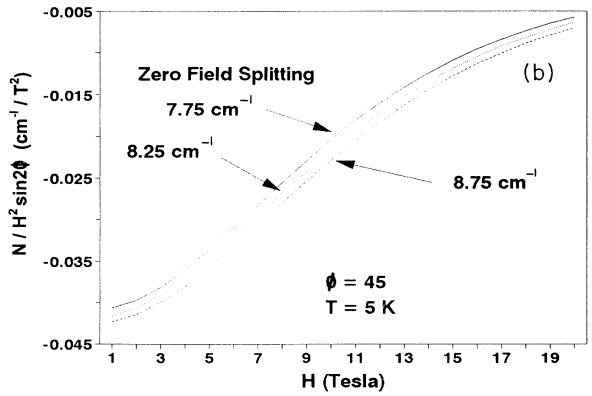

FIG. 5. Dependence of $\overline{M}_x/H_x$, $\overline{M}_z/H_z$, and $N/H^2\sin 2\phi$ upon the zero-field splitting δ.

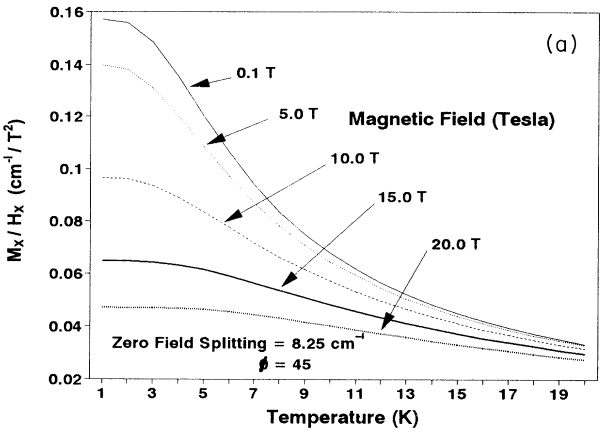

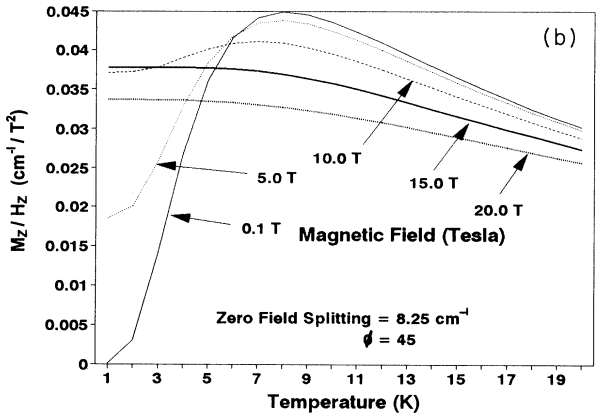

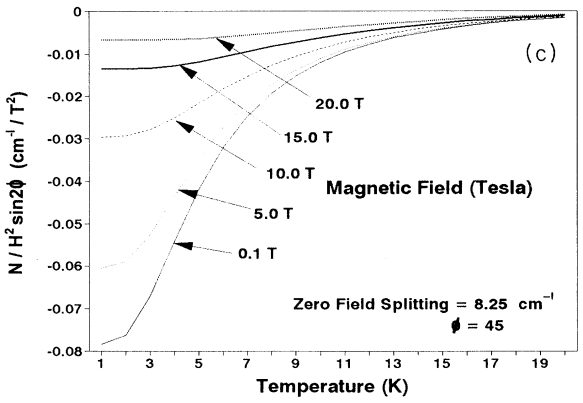

FIG. 6. Dependence of $\overline{M}_x/H_x$, $\overline{M}_z/H_z$, and $N/H^2\sin 2\phi$ upon temperature for field strengths from 0.1 to 20 T.

TABLE I. Magnetic-susceptibility tensor elements for V^{3+}:Al_2O_3 from Eq. (11) for $T=5$, 15, and 77 K with $\delta=8.25\ cm^{-1}$.

	5 K	15 K	77 K
χ_{xx}	1.20×10^{-1} cm^{-1}/T^2	4.50×10^{-2} cm^{-1}/T^2	8.27×10^{-3} cm^{-1}/T^2
χ_{xxxx}	-1.23×10^{-3} cm^{-1}/T^4	-1.94×10^{-4} cm^{-1}/T^4	-3.67×10^{-5} cm^{-1}/T^4
χ_{xxzz}	3.47×10^{-5} cm^{-1}/T^4	-3.41×10^{-5} cm^{-1}/T^4	-3.59×10^{-7} cm^{-1}/T^4
χ_{xxxxxx}	2.28×10^{-5} cm^{-1}/T^6	5.34×10^{-6} cm^{-1}/T^6	1.08×10^{-6} cm^{-1}/T^6
χ_{zz}	3.61×10^{-2} cm^{-1}/T^2	3.65×10^{-2} cm^{-1}/T^2	9.43×10^{-3} cm^{-1}/T^2
χ_{zzzz}	2.11×10^{-4} cm^{-1}/T^4	-1.91×10^{-5} cm^{-1}/T^4	-3.93×10^{-7} cm^{-1}/T^4
χ_{zxxz}	3.47×10^{-5} cm^{-1}/T^4	-3.41×10^{-5} cm^{-1}/T^4	-3.59×10^{-7} cm^{-1}/T^4

CONCLUSIONS

In the previous sections we have calculated the effects of high-field magnetic-induced anisotropy and saturation on the temperature-dependent magnetizations $\overline{M}_x$ and $\overline{M}_z$ and on the magnetic torque N for the V^{3+}:Al_2O_3 system. To illustrate the behavior and the magnitude of the anisotropy, the approximate susceptibility terms from Eq. (11) have been evaluated at $T=5$ and 77 K and are reported in Table I. These coefficients give a good qualitative and semiquantitive indication of the effects that are reported more rigorously in the graphs of the previous section.

First, the quartic terms in the susceptibility tensor are at least two orders of magnitude smaller than the leading quadratic terms. Second, the diagonal quartic terms χ_{xxxx} and χ_{zzzz} are again 50 times larger than the off-diagonal elements χ_{xxzz} and χ_{zxxz} at low temperatures. Third, some of the quartic terms change sign between 5 and 15 K. In general, at 1 T or less, the quadratic susceptibility terms give the desired magnetization to better than 1%. However, at 4 T and 5 K, χ_{xxxx} contributes to $\overline{M}_x$ 16% of χ_{xx}, χ_{xxxxxx} 4% of χ_{xx}, χ_{zzzz} 10% of χ_{zz} to $\overline{M}_z$, χ_{xxzz} 1% of χ_{xx}, and χ_{zxxz} 2% of χ_{zz}. The relative contributions are smaller at 4T and 77 K for $\overline{M}_x$.

Therefore, the most significant effects illustrated in Figs. 3–6 are for the most part due to saturation. The saturation effects are strongly field dependent and this is illustrated clearly in Fig. 6 where $\overline{M}_x/H_x$, etc., are graphed as a function of temperature. At the same time, the dependence of $\overline{M}_x/H_x$, etc., upon orientation of the crystal with respect to the magnetic field are substantial as indicated in Fig. 4. At low temperatures, 5 K, this effect becomes prominent at 3 T and increases to a maximum at 11 T. This effect vanishes altogether for fields less than 1 T and also with increasing temperature.

Finally, we have been especially concerned with the sensitivity of the high-field anisotropy and saturation to the zero-field splitting δ. In our work of some years ago, our weak-field, low-temperature susceptibility measurements[1(a)] gave $\delta=8.4\ cm^{-1}$. We arbitrarily put error bars on as $\pm0.2\ cm^{-1}$. A few years later Joyce and Richards[6] used infrared spectroscopic techniques and obtained $\delta=8.25\ cm^{-1}$ from spectral line splittings. Further, they measured the spectral effects as a function of magnetic field for the field along the perpendicular to the trigonal axis. Our calculations from Fig. 5 show that the dependence of $\overline{M}_x$ and $\overline{M}_z$ upon δ is most pronounced at the low magnetic fields. At the same time the torque N shows the same dependence at low and high fields. Therefore, it is our opinion that magnetic measurements at high fields would give no further information on δ.

*Previous address: Department of Physics, Louisiana Tech University, Ruston, Louisiana 71272.

[1](a) W. Brumage, C. Quade, and C. Lin, Phys. Rev. **131**, 949 (1963); (b) C. Quade, W. Brumage, and C. Lin, J. Chem. Phys. **37**, 1368 (1962); (c) W. Brumage, C. Lin, and J. Van Vleck, Phys. Rev. **132**, 608 (1963); (d) W. Brumage, C. Yarger, and C. Lin, *ibid.* **133**, A765 (1964); (e) W. Brumage and C. Lin, *ibid.* **134**, A950 (1964); (f) W. Brumage, E. Segraves, and C. Lin, J. Chem. Phys. **42**, 3326 (1965); (g) J. Mahoney, C. Lin, and W. Brumage, *ibid.* **50**, 2263 (1969); (h) J. Mahoney, C. Lin, W. Brumage, and F. Dorman, *ibid.* **53**, 4286 (1970). The instruments used to measure the magnetic properties of several dilute magnetic materials were described in the above papers.

[2]M. Villeret, S. Rodriguez, E. Kartheuser, A. Camacho, and L. Quiroga, Phys. Rev. B **44**, 399 (1991); E. Kartheuser, S. Rodriguez, and M. Villeret, *ibid.* **48**, 14 127 (1993); these papers contain many additional references.

[3]T. Fries, Y. Shapria, A. Twardowski, E. McNuff, Jr., T. Q. Wu, R. Kershaw, K. Dwight, and A. Wold, Phys. Rev. B **49**, 11 870 (1994).

[4]G. M. Zerev and A. Prokhorov, Sov. Phys. JETP **7**, 707 (1958); **11**, 330 (1960); **13**, 714 (1961).

[5]J. H. Van Vleck, *The Theory of Electric and Magnetic Susceptibilities* (Oxford University Press, London, 1932), pp. 145, 182.

[6]R. Joyce and T. Richards, Phys. Rev. **179**, 375 (1969).